LAWRENCE
LIVERMORE
NATIONAL
LABORATORY

UCRL-PROC-216071

Inhibition of Chloride Induced Crevice Corrosion in Alloy 22 by Fluoride Ions

R. M. Carranza, M. A. Rodríguez, R. B.Rebak

October 11, 2005

Corrosion/2006 Conference and Exposition
San Diego, CA, United States
March 12, 2006 through March 16, 2006

Disclaimer

INHIBITION OF CHLORIDE INDUCED CREVICE CORROSION IN ALLOY 22 BY FLUORIDE IONS

Ricardo M. Carranza and Martín A. Rodríguez
Dep. Materiales, Comisión Nacional de Energía Atómica
Av. Gral. Paz 1499
B1650KNA San Martín, Buenos Aires, ARGENTINA

Raúl B. Rebak
Lawrence Livermore National Laboratory
7000 East Ave, L-631
Livermore, CA 94550, USA

ABSTRACT

Alloy 22 (N06022) is highly resistant to localized corrosion. Alloy 22 may be susceptible to crevice corrosion in pure chloride (Cl^-) solutions under aggressive environmental conditions. The effect of the fluoride (F^-) over the crevice corrosion induced by chloride ions is still not well established. The objective of the present work was to explore the crevice corrosion resistance of this alloy to different mixtures of fluorides and chlorides.

Cyclic potentiodynamic polarization (CPP) tests were conducted in deaerated aqueous solutions of pure halide ions and also in different mixtures of chloride and fluoride at 90°C and pH 6. The range of chloride concentration $[Cl^-]$ was $0.001\ M \leq [Cl^-] \leq 1\ M$ and the range of molar fluoride to chloride ratio $[F^-]/[Cl^-]$ was $0.1 \leq [F^-]/[Cl^-] \leq 10$.

Results showed that Alloy 22 was susceptible to crevice corrosion in all the pure chloride solutions but not in the pure fluoride solutions. Fluoride ions showed an inhibitor behavior only in mixtures with a molar ratio $[F^-]/[Cl^-] > 2$. For mixtures with a molar ratio $[F^-]/[Cl^-]$ of 7 and 10 the inhibition of crevice corrosion was complete.

Keywords: N06022, chloride, fluoride, inhibition, crevice corrosion, repassivation potential, cyclic polarization

INTRODUCTION

Alloy 22 (N06022) is nickel (Ni) based and contains nominally 22% Chromium (Cr), 13% Molybdenum (Mo) and 3% tungsten (W)[1]. Alloy 22 is one of the most versatile alloys of the Ni-Cr-Mo family and was designed to withstand the most aggressive industrial applications, including reducing acids such as hydrochloric and oxidizing acids such as nitric[2]. The base element (nickel) is very resistant to hot alkalies, and the alloying elements chromium and molybdenum enhance its protection against oxidizing and reducing conditions respectively[2,3,4]. Alloy 22 has showed excellent resistance to pitting, crevice corrosion and environmentally assisted cracking in hot concentrated chloride solutions[2,3,4]. Applications of Alloy 22 include a variety of chemical processing, pickling and metal finishing, pollution control, nuclear waste treatment and pulp and paper industry[3,4], but the widest applications is in flue-gas desulfurization (FGD) plants[5]. Due to its excellent performance in a wide variety of environments Alloy 22 has been selected for the fabrication of the corrosion-resistant outer shell of the high-level nuclear waste container for the proposed Yucca Mountain repository[6].

Alloy 22 can be considered not susceptible to pitting corrosion in practical applications in chloride containing environments[2]. However, Alloy 22 might suffer crevice corrosion under certain aggressive conditions[2]. The factors influencing crevice corrosion susceptibility of Alloy 22 can be classified into environmental (external) and metallurgical (internal) [6,7]. External factors include[7] chloride concentration, temperature, applied potential, presence of inhibitors or deleterious species, pH, microbial activity, volume of electrolyte, crevice former geometry, crevicing material, etc. Internal factors include[7] the metallurgical condition of the alloy (microstructure), presence of a weld seam, type of annealing, oxide film formed, surface finishing, etc. A more detailed discussion regarding this topic can be found elsewhere[7]. Many of the factors listed above, such as chloride concentration, temperature and inhibitors (namely nitrate and sulfate) have been studied in some detail[6,8,9,10,11]. The influences of other factors still need to be investigated[7]. In particular the role of halides other than chloride is still not well established[7,12,13,14,15,16,17] and will be briefly discussed in this paper.

Meck *et al*. did not find crevice corrosion in prismatic Alloy 22 specimens (ASTM G 5) tested in 1 M NaCl pH 6 and in 1 M NaF pH 9 solutions at 50°C[12]. They found similar passive current densities in both solutions but some differences in the breakdown potential (E_{20}) that were mainly attributed to a difference in the pH of the electrolytes[12]. Meck *et al*. also tested Multiple Crevice Assemblies (MCA) Alloy 22 specimens (ASTM G 48) in 1 M NaCl pH 6, 1 M NaF pH 9 and 0.5 M NaCl + 0.5 M NaF pH 8 at 60ºC and 90ºC[12]. None of the specimens tested in 1 M NaF solution suffered crevice corrosion[12]. Crevice corrosion was detected in 0.5 M NaCl + 0.5 M NaF solution at both temperatures and in 1 M NaCl solution only at 90ºC[12]. These results are consistent with those found by Rodríguez *et al*. who performed CPP tests in prismatic Alloy 22 specimens at 90ºC in the same solutions[14]. Dunn *et al*. tested the influence of fluoride ions when added to 0.5 M NaCl solutions at 95°C for thermally aged Alloy 22 probes (5 min at 870°C)[16]. They used fluoride to chloride ratios ranging from 0.2 to 0.8 and reported that fluoride anion was not an inhibitor to crevice corrosion as found for oxyanions such as nitrate, sulfate, carbonate and bicarbonate[16]. Rodríguez *et al*. tested the corrosion susceptibility of prismatic specimens of Mill Annealed (MA) and thermally aged Alloy 22 in 1 M NaF solutions at pH 6, 7.3 and 9 and 90ºC[13]. Thermal aging was performed to create conditions of full aging with Topologically Closed Packed phases (TCP or 10 h at 760°C) and Long Range Ordering (LRO or 1000 h at 538°C). Neither pitting nor crevice corrosion was detected in any of the tested conditions even though the specimens were polarized to anodic potentials where cur-

rent densities of up to 10 mA/cm² were applied[13]. Rodríguez *et al*. also performed electrochemical tests for prismatic specimens of Alloy 22 under the same metallurgical conditions in 1 M NaCl pH 2, 6 and 9 and 0.5 M NaCl + 0.5 M NaF at pH 6 and 9[15]. Comparing their results with the 1 M NaF results[13] they concluded that Alloy 22 seemed more susceptible to crevice corrosion in the mixed halide solution than in the pure 1 M NaCl solution of the same pH[15], but was immune to crevice corrosion in pure1 M NaF solution.

Very limited studies exist regarding the effect of bromide (Br^-) ions on the localized corrosion of Alloy 22. Rebak *et al*. performed cyclic potentiodynamic polarization (CPP) tests in 1 M NaCl and 1 M NaBr solutions at 50°C[17]. Both solutions had a similar pH of approximately 6. Alloy 22 did not suffer either crevice or pitting corrosion in neither solution[17]. It has been reported that alloying elements such as Mo, which are highly beneficial for protection against localized corrosion in chloride solutions may not be as efficient in bromide containing solutions[17].

The aim of the present work was to establish the effect of the fluoride ion on the chloride induced crevice corrosion of Alloy 22 at 90°C.

EXPERIMENTAL PROCEDURE

Alloy 22 (N06022) specimens were prepared from wrought mill annealed plate stock. The chemical composition of the alloy in weight percent was 59.56% Ni, 20.38% Cr, 13.82% Mo, 2.64% W, 2.85% Fe, 0.17% V and 0.16% Mn (Heat 059902LL1). All the tested material was wrought Mill Annealed (MA). The specimens were prism crevice assemblies (PCA), which were fabricated based on the washer for crevice forming described in ASTM G 48[1]. The PCA specimen has been described before[1]. The tested surface areas were approximately 14 cm². The specimens had a finished grinding of abrasive paper number 600 and were degreased in acetone and washed in distilled water 1 hour prior to testing.

Electrochemical tests were performed in deaerated halide solutions at 90°C. These included (a) pure chloride solutions 0.001 M-1 M NaCl, (b) pure fluoride solutions NaF saturated at room temperature (approximately 1 M NaF), and (c) halide mixtures (chloride plus fluoride solutions). The halide mixtures consisted in sodium salts (x M NaCl + y M NaF) or potassium salts (x M KCl + y M KF). The range of chloride concentration $x = [Cl^-]$ was $0.001\ M \leq x \leq 1\ M$ and the range of molar fluoride to chloride ratio $y/x = [F^-]/[Cl^-]$ was $0.1 \leq y/x \leq 10$. The potassium salts were used only for the most concentrated solutions in order to avoid precipitation of the less soluble fluoride salts. The pH of these solutions was fixed at 6 by additions of small volumes of NaOH, HCl or HF. The pH of the more dilute solutions ($[Cl^-] < 0.01$ M) was not fixed in order to avoid changing the halide concentration, but the natural pH of these solutions was near 6 (not less than 5.6). The pH of the solutions was measured at the end of each test. Nitrogen (N_2) was purged through the solution 1 hour prior to testing and was continued throughout the entire test. The electrochemical tests were conducted in two types of one-liter, three-electrode vessels (ASTM G 5)[1]. The former was a traditional borosilicate glass vessel and the latter was a stainless steel PTFE-coated vessel. This second type of vessel was used in order to avoid glass dissolution in fluoride containing media. A water-cooled condenser combined with a water trap was used to avoid evaporation of the solution and to prevent the ingress of air (oxygen). The temperature of the solution was controlled by immersing the cell in a thermostatized bath, which was kept at a constant temperature. All the tests were performed at ambient pressure. The reference electrode was a saturated calomel electrode (SCE), which has a potential of 0.242 V more positive than the standard hydrogen electrode (SHE). The reference

electrode was connected to the solution through an air-cooled Luggin probe. The tip of the Luggin probe in contact with the solution was made of PTFE, but the upper part in contact with the reference electrode was made of borosilicate glass. The counter electrode consisted in two connected flags of platinum foil (total area 100 cm^2) spot-welded to a platinum wire. All the potentials in this paper are reported in the SCE scale.

Cyclic potentiodynamic polarization (CPP) tests (ASTM G 61)[1] were performed. The potential scan was started 0.150 V below the corrosion potential (E_{CORR}) in the anodic direction at a scan rate of 0.167 mV/s. The scan direction was reversed when the current density reached 1-10 mA/cm^2 in the forward scan or when the potential reach a value of 0.850 V_{SCE} (the first occurring event). A potentiostatic hold was performed for 5 minutes at the onset potential (0.150 V below E_{CORR}) before starting the scan. After the CPP tests, the specimens were examined in an optical microscope (OM) to establish the mode, location and depth of the attack. Some of the specimens were observed in the scanning electron microscope (SEM).

RESULTS

Figure 1 shows cyclic potentiodynamic polarization curves for Alloy 22 specimens in NaCl solutions of different concentrations at pH 6 and 90ºC. A wide range of passivity was observed in all cases and the passive current seemed to be independent of the chloride concentration of the solution (Figure 1). The four specimens suffered different degrees of crevice corrosion under the crevice formers. Hysteresis in the reverse scan was associated with this phenomenon. Pitting corrosion was not observed in any case. Critical parameters for crevice corrosion, namely breakdown and repassivation potentials, can be extracted from these CPP tests (Table 1). The criteria used in the present work are listed below[2,10].

Breakdown potential: E_{20} is the potential at which the current density reaches 20 $\mu A/cm^2$ in the forward scan.

Repassivation potential: (I) E_{R1} is the potential at which the current density reaches 1 $\mu A/cm^2$ in the reverse scan, and (II) E_{CO} (cross over potential) is the potential at which the reverse scan intersects the forward scan.

Figure 2 shows the critical parameters (E_{20}, E_{R1} and E_{CO}) as a function of chloride concentration $[Cl^-]$ of the solution. The three parameters decreased as the chloride concentration increased (Figure 2). The breakdown potential (E_{20}) was determined by the onset of crevice corrosion for $[Cl^-]$ = 1 M and $[Cl^-]$ = 0.5 M, as long as the onset of transpassivity occurs at higher potentials (~0.500 V_{SCE}) in pH 6 chloride solutions[15]. For $[Cl^-]$ = 0.1 M-0.001 M the passivity breakdown potential could have been influenced both by crevice corrosion and by transpassivity onset. Both repassivation potentials criteria (E_{R1} and E_{CO}) lead to the same values in the entire measurement range (Figure 2). It was due to the fact that the passive current density was almost the same and near 1 $\mu A/cm^2$ for all pure chloride solutions.

A linear decrease of repassivation potential as chloride concentration increases logarithmically ($E = -A - B \log [Cl^-]$) was found as reported elsewhere[7]. The results of linear least squares fits for both criteria and the correlation coefficients (R^2) are listed below.

$$E_{R1} = -0.127 - 0.056 \log [Cl^-] \qquad R^2 = 0.959 \qquad (1)$$

$$E_{CO} = -0.125 - 0.050 \log [Cl^-] \qquad R^2 = 0.953 \qquad (2)$$

Statistical dispersion of the critical parameters was calculated with the four CPP tests performed in 1 M NaCl at pH 6 and 90ºC. Individual values of the four considered CPP curves are listed in Table 1. The average values were: E_{20} = 0.216 V_{SCE}, E_{R1} = –0.139 V_{SCE} and E_{CO} = –0.139 V_{SCE}. The corresponding standard deviations were 0.100 V (E_{20}) 0.008 V (E_{R1}) and 0.014 V (E_{CO}). These values indicate that E_{20} showed a wider dispersion while E_{R1} and E_{CO} showed a narrower dispersion.

Figure 3 shows two CPP performed out in 1 M NaF solutions at pH 6 and 90ºC. One of them was performed in a traditional borosilicate glass vessel and the other in a stainless steel PTFE-coated vessel in order to evaluate the effect of glass dissolution on the corrosion behavior of Alloy 22 and thus compare with previous measurements performed in glass vessels[12,13]. The CPP test performed in the glass vessel showed an anodic peak (Figure 3) in the transpassive potential range (~0.500 V_{SCE}). Contrarily, the one performed in the PTFE-coated vessel showed a sustained increase in current as the potential increased (Figure 3). At the end of the experiment performed in the glass vessel a yellowish gelatinous precipitate was found in the solution and deposited on the specimen as described elsewhere[13]. In the experiment performed in the PTFE-coated vessel no precipitate was found. Neither crevice corrosion nor pitting corrosion was observed in any case in these pure fluoride solutions. All the other CPP curves performed in fluoride containing solutions were performed in the stainless steel PTFE-coated vessel.

Figure 4 shows CPP performed out in 0.1 M Cl^- (NaCl or KCl) solutions at pH 6 and 90ºC with fluoride contents ranging from 0.01 M to 1 M. As the fluoride concentration increased passivity current density also increased. The increase in current density after passivity breakdown was sharper the higher was the fluoride concentration. Considerable hysteresis was observed between the forward and reverse scan in the solutions of lower fluoride concentration (with 0.01 M NaF and 0.1 M NaF) but a small or negligible hysteresis was observed in the solutions of higher fluoride concentration (with 0.7 M NaF and 1 M KF). The specimen tested in the solution of the highest fluoride concentration (with 1 M KF) did not suffer crevice corrosion. The specimens tested in the other three solutions suffered different degrees of localized attack under the crevice formers. Figure 5 shows CPP curves performed in 1 M Cl^- (NaCl or KCl) solutions at pH 6 and 90ºC with fluoride contents ranging from 0.1 M to 5 M. An important increase of passive current density with fluoride concentration was also observed. Hysteresis was observed between the forward and the reverse scan in all solutions but it was larger for the solutions of lower fluoride concentration (with 0.1 M NaF and 1 M KF). All the specimens suffered crevice corrosion. The curve corresponding to the solution 5 M KF + 1 M KCl showed an anodic peak similar to the peak detected previously in CPP tests performed in 1 M NaF in the glass vessel (Figure 3 and Reference 13). This fact will be discussed in the next section. Pitting corrosion was not observed in any case.

A single criterion for determining the repassivation potential (*i.e*: E_{R1} or E_{CO}) should be selected in order to compare the crevice corrosion susceptibility of Alloy 22 when tested in different halide mixtures. The significant variability of the passive current density with the fluoride concentration (Figures 4 and 5) could hinder any inhibitive effect of fluoride ion if E_{R1} is taken as a criterion, so the chosen criterion was the cross over potential (E_{CO}). The critical parameters extracted from each CPP test (E_{20}, E_{R1} and E_{CO}) are listed in Table 1.

Figure 6 shows the cross over repassivation potentials for crevice corrosion (E_{CO}) for Alloy 22 as a function of chloride concentration [Cl^-], for different fluoride to chloride molar ratio [F^-]/[Cl^-] at pH 6 and 90ºC. E_{CO} decreased with [Cl^-] and increased with [F^-]/[Cl^-] (Figure 6). A

threshold molar ratio $[F^-]/[Cl^-] = 2$ was required in order to obtain a significant increase in E_{CO} (Figure 6). For a ratio $[F^-]/[Cl^-] = 7$ crevice corrosion damage was negligible in most cases, and for a ratio $[F^-]/[Cl^-] = 10$ crevice corrosion was not observed. The threshold molar ratio $[F^-]/[Cl^-]$ for a complete inhibition was between 5 and 10. For $[Cl^-] = 0.01$ M a threshold molar ratio of $[F^-]/[Cl^-] = 5$ was enough for the inhibition to be complete, but for $[Cl^-] = 0.1$ M a threshold molar ratio of $[F^-]/[Cl^-] = 10$ was required. It suggests that this threshold molar ratio is higher the higher is the chloride concentration.

Crevice corrosion, when it occurred, appeared as a localized attack under the crevice formers (Figures 7,8,9). The type of attack was described as crystalline[7]. In many cases the grains of the alloy are discernible as well as crystal planes in scanning electron microscope images (Figures 10,11). This attack seems to follow the higher energy planes in the crystal structure of the grains[7]. The maximum depths of attack detected by optical microscopic observation for each test and other relevant information are listed in Table 1. As a general observation, the depth of attack was higher for higher chloride concentrations and for lower fluoride to chloride molar ratios (Table 1). The part of the specimens boldly exposed to the solution (not occluded area) suffered transpassive dissolution which was detected as a discolored oxide (Figure 7). The specimens tested in high fluoride concentration solutions ($[F^-] > 2$ M) presented a green precipitate deposited on them (Figure 8). It could be deposited silica due to glass dissolution from reference electrode and from the upper part of the Luggin-probe and it was also associated with an anodic peak in the corresponding CPP test at transpassivity potentials. As the solutions used in these work were not buffered, some changes in the pH value were detected at the end of each CPP test (Table 1).

DISCUSSION

The relationships obtained for the critical parameters (E_{20}, E_{R1} and E_{CO}) with the chloride concentration of the solution were similar to those reported elsewhere[7]. The statistical dispersion of repassivation potentials was narrow but it was only tested for a chloride concentrated solution (1 M). It should be tested for less concentrated solutions (less aggressive) because the statistical dispersion of these parameters is thought to increase for less aggressive media[18].

Although the detrimental effect of fluoride ions on glass dissolution[19] is well known, most of the electrochemical tests of Ni-Cr-Mo alloys in fluoride containing media reported in literature were performed in conventional borosilicate glass vessels[12,13,14,15,16,21,22,23,24]. Presence of an anodic peak in the transpassivity potential region observed in those CPP tests performed in fluoride solutions contained in glass vessels[13,15] (Figure 3) or even in fluoride solutions in contact with small glass areas (Figure 5) could be attributed to the inhibitive effect of dissolved silica which is deposited on the surface of the alloy. Silicon exerts a beneficial effect in Ni-Cr-Si alloys when they are tested in super-oxidizing media (*e.g.* concentrated sulfuric acid) by preventing chromium transpassivity[20]. It was attributed to the development of a pseudo-passive film enriched in silica[20]. Further research is needed to elucidate the effect of silica deposits on the transpassive dissolution and also on crevice corrosion susceptibility of Alloy 22. It would be especially important for the performance of the nuclear waste container for the proposed Yucca Mountain repository as the surrounding environment is formed by rocks which can decompose into silica[6]. It is important to point out that CPP curves performed in simulated concentrated well water (SCW)[6] of Yucca Mountain, which has a fluoride concentration of approximately 0.074 M, present also an anodic peak[21,22,23,24]. Although it was attributed to the

presence of bicarbonate[23,24], the dissolution of silica from the vessel enhanced by the presence of fluoride ions could cause a similar effect.

Passive current density did not show any significant dependence with chloride concentration of the solution in pure chloride media (Figure 1) but showed an important dependence with fluoride concentration (Figures 4 and 5) in the mixed halide media. Transpassive current seemed to be also more affected by the fluoride concentration of the solution (Figures 4 and 5) than by the chloride concentration (Figure 1). It has been reported that fluoride ion is able to incorporate to the passive oxide film at sites previously occupied by oxygen thus decreasing the film stability[25]. Incorporation of chloride ions to the oxide lattice is limited by its larger ionic radius. Possibility of strong metal complexes formation (with Ni^{2+} and Cr^{3+}) should be taken into account in explaining these observations[26]. The reported equilibrium constants for metal-fluoride complexes are orders of magnitude higher than for metal-chloride complexes[26]. Further studies are needed to elucidate this issue.

Based on studies in nickel (Ni) and iron (Fe), B. R. MacDougall point out, that chloride is more dangerous for localized corrosion while fluoride enhance general corrosion, and in combination they are potentially even more dangerous[25]. G. A. Cragnolino also sustains the same hypothesis.[18] They suggest that fluoride could enhance the deleterious effect of chloride on the crevice corrosion of Alloy 22. On the other hand, R. C. Newman sustains that fluoride is not an aggressive species for localized corrosion of stainless steel and since HF is a weak acid[(1)], fluoride could act as an inhibitor of pitting and crevice corrosion of stainless steels and Ni-Cr-Mo alloys[27]. Researches carried out by Meck *et al*.[12], Dunn *et al*.[16] and Rodríguez *et al*.[15] did not show any inhibitive effect of fluoride ions on the chloride induced crevice corrosion of Alloy 22. Contrarily, they suggested that the addition of fluoride to chloride solutions may be detrimental to the passive film breakdown.

According to the results presented in this paper and information reviewed[7,12,13,14,15,16] about the crevice corrosion susceptibility of Alloy 22 in chloride and fluoride mixtures, it can be concluded that fluoride behaves as a weak inhibitor of chloride induced crevice corrosion of Alloy 22. The most well known inhibitors for this system are oxyanions such as nitrate, sulfate, carbonate and bicarbonate[6,7,8,9,10,11,16]. These anions lead to a complete inhibition of chloride induced crevice corrosion of Alloy 22 for molar inhibitor to chloride ratios of 0.1-0.5 in experimental conditions similar to those used in the present work[6,7,8,9,10,11,16]. The molar fluoride to chloride ratio required for a complete inhibition of crevice corrosion was at least one order of magnitude higher. This high fluoride to chloride ratio along with detrimental effects of fluoride on passivity and transpassivity (*i.e.* general corrosion) of Alloy 22 in previous studies overshadowed the inhibitive effect of fluoride ion on the chloride induced crevice corrosion[7,12,14,15,16]. All the tests performed previously used fluoride to chloride ratios ranging from 0.2 to 1. None inhibitive effect was found for such a low ratios as it was also shown in the present work.

Further research proposed by the authors include potentiostatic tests at a constant chloride concentration (*e.g.* $[Cl^-] = 0.1M$) with fluoride to chloride molar ratios ranging from 0.1 to 10 at a fixed potential higher than the repassivation potential of the corresponding pure chloride solution (in this example $E > E_{CO} = -0.070\ V_{SCE}$). Monitoring of current density over time will help to establish the effect of fluoride ion on induction time for the onset of crevice corrosion and crevice corrosion current density.

[1] Hydrofluoric acid (HF) would be one of the main species inside a crevice in a fluoride containing solution.

CONCLUSIONS

1. The breakdown (E_{20}) and repassivation (E_{R1} and E_{CO}) potentials for Alloy 22 in pure chloride solution decreased with chloride concentration showing a relationship of the type $E = -A - B \log [Cl^-]$.

2. The cross over repassivation potential (E_{CO}) for Alloy 22 in chloride and fluoride mixtures decreased with chloride concentration and increased with fluoride to chloride molar ratio.

3. Fluoride behaved as an inhibitor of chloride induced crevice corrosion of Alloy 22 in the studied conditions.

4. A fluoride to chloride molar ratio from 5 to 10 was required for the inhibition to be complete at pH 6 and 90ºC.

5. There was a moderate or negligible inhibitive effect for fluoride to chloride molar ratios less than 2.

AKNOWLEDGEMENTS

This work was performed under the auspices of the U. S. Department of Energy (DOE) by the University of California Lawrence Livermore National Laboratory under contract N° W-7405-Eng-48, and supported by the Yucca Mountain Project, which is part of the Office of Civilian Radioactive Waste Management (OCRWM).

R. M. Carranza acknowledges financial support from the Agencia Nacional de Promoción Científica y Tecnológica of the Ministerio de Educación, Ciencia y Tecnología from Argentina.

DISCLAIMER

REFERENCES

1 ASTM International, Annual Book of ASTM Standards, Volume 03.02 “Corrosion of Metals” (West Conshohocken, PA: ASTM International, 2002).

2 R. B. Rebak in Corrosion and Environmental Degradation, Volume II, (Wiley-VCH, 2000: Weinheim, Germany).

3 A. I. Asphahani, The Arabian Journal of Science and Engineering Vol. 14, Nº2 pp. 317-335 (1989).

4 P. E. Manning, J. D. Smith, and J. L. Nickerson, Materials Performance, pp. 67-73, June 1988.

5 A. Boniface, The Chemical Engineer, No. 477, p. 21 (July 1990).

6 G. M. Gordon, Corrosion, 58, p. 811 (2002).

7 R. B. Rebak, Paper 05610 Corrosion/2005, NACE Intl. 2005: Houston, TX.

8 B. A. Kehler, G. O. Ilevbare and J. C. Scully, Corrosion, p. 1042 (2001).

9 K. J. Evans, and R. B. Rebak, Corrosion Science a Retrospective and Current Status in Honor of R. P. Frankenthal, The Electrochemical Society 2002, Pennington, New Jersey, 2002-13, pp. 344-354.

10 R. B. Rebak and J. C. Estill in Fall Meeting of the Materials Research Society, Boston, Massachusetts, 2-6 December 2002, Vol. **757**, Paper II4.1, pp 713-721.

11 D. S. Dunn, Y.-M. Pan, K. Chiang, L. Yang, G. A Cragnolino and X. He "Localized Corrosion Resistance and Mechanical Properties of Alloy 22 Waste Package Outer Containers" JOM, January 2005, pp 49-55.

12 N. S. Meck, P. Crook, S. D. Day, and R. B. Rebak, Paper 03682, Corrosion/03 NACE Intl. 2003, Houston, TX.

13 M. A. Rodríguez, R. M. Carranza and R. B. Rebak, Paper 04700, Corrosion/04, NACE Intl. 2004, Houston, TX.

14 M. A. Rodríguez, R. M. Carranza, S. D. Day and R. B. Rebak, Paper 05599, Corrosion/05, NACE Intl. 2005, Houston, TX.

15 M. A. Rodríguez, R. M. Carranza and R. B. Rebak, Met. Trans. A Vol. **36A**-No.5, 2005, pp. 1179-1185.

16 D. S. Dunn, L. Yang, C. Wu and G. A. Cragnolino, Mat. Res. Soc. Symp. Proc. Vol 824 (MRS, 2004: Warrendale, PA)

17 R. B. Rebak, N. E. Koon, J. P. Cotner and P. Crook, ECS PV 99-27, p. 473 (The Electrochemical Society, 1999: Pennington, NJ)

18 G. A. Cragnolino in Proceedings from an Intl. Workshop on Long-Term Passive Behavior, 19 and 20 July, Arlington, Virginia, ed. A. A. Sagüés and C. A. W. Di Bella, USNWTRB, 2001, pp. 11-16.

19 I. M. Kolthoff, E. B. Sandell, E. J. Meehan and S. Bruckenstein - Análisis Químico Cuantitativo -Librería y Editorial Nigar S. R. L., Buenos Aires, Cuarta Edición, 1972.

20 Haynes International - Guide to corrosion-resistant nickel alloys - H-2114B (2002).

21 G.O. Ilevbare, T. Lian and J.C. Farmer, Paper 02539, Corrosion/02, NACE Intl. 2002, Houston, TX.

22 R. B. Rebak, T. S. E. Summers, T. Lian, R. M. Carranza, J. R. Dillman, T. Corbin and P. Crook, Paper 02542, Corrosion/02, NACE Intl. 2002, Houston, TX.

23 K. T. Chiang, D. S. Dunn, and G. A. Cragnolino, Paper 02463, Corrosion/05, NACE Intl. 2005, Houston, TX.

24 P. J. Bedrossian, Potential-Dependence of the Aqueous Oxidation of Alloy 22 in Simulated Concentrated Well Water, U. S. Department of Energy Lawrence Livermore National Laboratory, UCRL-ID-142349, 2000 (http://www.llnl.gov/tid/Library.html).

25 B. R. MacDougall in Proceedings from an Intl. Workshop on Long-Term Passive Behavior, 19 and 20 July, Arlington, Virginia, ed. A. A. Sagüés and C. A. W. Di Bella, USNWTRB, 2001, pp. 49-54.

26 R. M. Smith and A. E. Martell, Critical Stability Constants, 1976 Plenum Press New York, Vol. 3 Inorganic Complexes.

27 R. C. Newman, Waste Package Materials Performance Peer Review, A Compilation of Special Topic Reports (Topic 10), Compiled and Edited by F. M. G. Wong and J. H. Prayer, 2002.

TABLE 1

CRITICAL PARAMETERS AND RELEVANT INFORMATION EXTRACTED FROM CPP TESTS.

Test	Solution	Molar $[F^-]/[Cl^-]$	E_{20}, V_{SCE}	E_{R1}, V_{SCE}	E_{CO}, V_{SCE}	Final pH	TC, A/cm^2	MDA, μm (± 5 μm)
NaCl101	1M NaCl	0	0.296	-0.144	-0.134	NA	1	120
NaCl102	1M NaCl	0	0.092	-0.128	-0.126	NA	1	150
NaCl103	1M NaCl	0	0.331	-0.135	-0.132	7.6	1	NA
NaCl106	1M NaCl	0	0.143	-0.149	-0.163	7.5	1	140
NaCl0501	0.5M NaCl	0	0.230	-0.102	-0.103	4.5	1	85
NaCl0101	0.1M NaCl	0	0.431	-0.055	-0.056	5.0	1	190
NaCl00101	0.01M NaCl	0	0.425	-0.033	-0.037	6.4	< 1 (0.85 V_{SCE})	45
NaCl000101	0.001M NaCl	0	0.507	0.048	0.026	6.2	< 1 (0.85 V_{SCE})	15
NaF103 (*PTFE)	1M NaF	no Cl^-	0.384	0.282	0.342	6.2	10	no crevice
NaF104 (**Glass)	1M NaF	no Cl^-	0.363	0.168	0.182	6.2	10	no crevice
NaF01Cl102	0.1M NaF+ 1M NaCl	0.1	0.376	-0.139	-0.136	6.5	10	80
KF1Cl101	1M KF+ 1M KCl	1	0.171	-0.155	-0.107	6.3	10	110
KF2Cl102	2M KF+ 1M KCl	2	0.111	-0.146	-0.076	6.5	0.85 V_{SCE}	130
KF5Cl101	5M KF+ 1M KCl	5	0.230	-0.283	-0.079	6.8	0.85 V_{SCE}	40
NaFCl0501	0.5M NaF+ 0.5M NaCl	1	0.285	-0.131	-0.080	6.7	10	135
NaF1KCl0501	1M NaF+ 0.5M KCl	2	0.387	-0.102	-0.036	6.3	10	50
KF25Cl0501	2.5M KF+ 0.5M KCl	5	0.330	-0.310	0.015	6.4	10	40
KF35Cl0501	3.5M KF+ 0.5M KCl	7	0.349	0.109	0.159	6.7	< 10 (1 V_{SCE})	40
NaF1KCl0201	1M NaF+ 0.2M KCl	5	0.386	-0.072	0.053	6.3	10	30
NaF001Cl0101	0.01M NaF+ 0.1M NaCl	0.1	0.364	-0.014	-0.033	6.6	< 10 (0.85 V_{SCE})	80
NaF01Cl0102	0.1M NaF+ 0.1M NaCl	1	0.376	-0.021	-0.036	6.3	10	90
NaF02Cl0101	0.2M NaF+ 0.1M NaCl	2	0.378	-0.088	-0.074	6.3	10	80
NaF02Cl0102	0.2M NaF+ 0.1M NaCl	2	0.393	-0.050	-0.044	6.4	10	40
NaF05Cl0102	0.5M NaF+ 0.1M NaCl	5	0.382	-0.121	0.073	6.7	10	75
NaF07Cl0101	0.7M NaF+ 0.1M NaCl	7	0.427	0.072	0.285	6.4	10	25
NaF1KCl0101	1M NaF+ 0.1M KCl	10	0.389	0.175	0.310	6.3	10	no crevice

TC = Threshold Current for Reversing Scan, MDA = Maximum Depth of Crevice Corrosion Attack, NA= Not Available, *PTFE = test performed in the PTFE-coated vessel, **Glass = test performed in the glass vessel. All the other tests in fluoride containing solutions were performed in the PTFE-coated vessel.

Test	Solution	Molar $[F^-]/[Cl^-]$	E_{20}, V_{SCE}	E_{R1}, V_{SCE}	E_{CO}, V_{SCE}	Final pH	TC, A/cm^2	MDA, μm (± 5 μm)
NaF001Cl00101	0.01M NaF+ 0.01M NaCl	1	0.408	0.029	-0.003	6.5	< 10 (0.85 V_{SCE})	15
NaF002Cl00101	0.02M NaF+ 0.01M NaCl	2	0.363	0.064	0.021	6.6	< 10 (0.85 V_{SCE})	105
NaF005Cl00102	0.05M NaF+ 0.01M NaCl	5	0.365	0.267	0.264	6.6	< 10 (0.85 V_{SCE})	no crevice
NaF007Cl00101	0.07M NaF+ 0.01M NaCl	7	0.36	0.266	0.269	6.6	< 10 (0.85 V_{SCE})	no crevice
NaF01Cl00102	0.1M NaF+ 0.01M NaCl	10	0.365	0.275	0.293	6.5	< 10 (0.85 V_{SCE})	no crevice
NaF0001Cl000101	0.001M NaF+ 0.001M NaCl	1	0.479	0.086	0.032	6.6	< 1 (0.85 V_{SCE})	15
NaF0002Cl000101	0.002M NaF+ 0.001M NaCl	2	0.468	0.225	0.232	6.4	< 1 (0.85 V_{SCE})	10
NaF0002Cl000102	0.002M NaF+ 0.001M NaCl	2	0.46	0.079	0.028	6.8	< 1 (0.85 V_{SCE})	10
NaF0005Cl000101	0.005M NaF+ 0.001M NaCl	5	0.454	0.241	0.216	5.9	< 1 (0.85 V_{SCE})	10
NaF0007Cl000101	0.007M NaF+ 0.001M NaCl	7	0.415	0.265	0.26	6.8	< 1 (0.85 V_{SCE})	no crevice
NaF001Cl000101	0.01M NaF+ 0.001M NaCl	10	0.411	0.196	0.155	6.7	< 1 (0.85 V_{SCE})	no crevice
NaF001Cl000102	0.01M NaF+ 0.001M NaCl	10	0.502	0.366	0.360	4.8	< 1 (0.85 V_{SCE})	no crevice

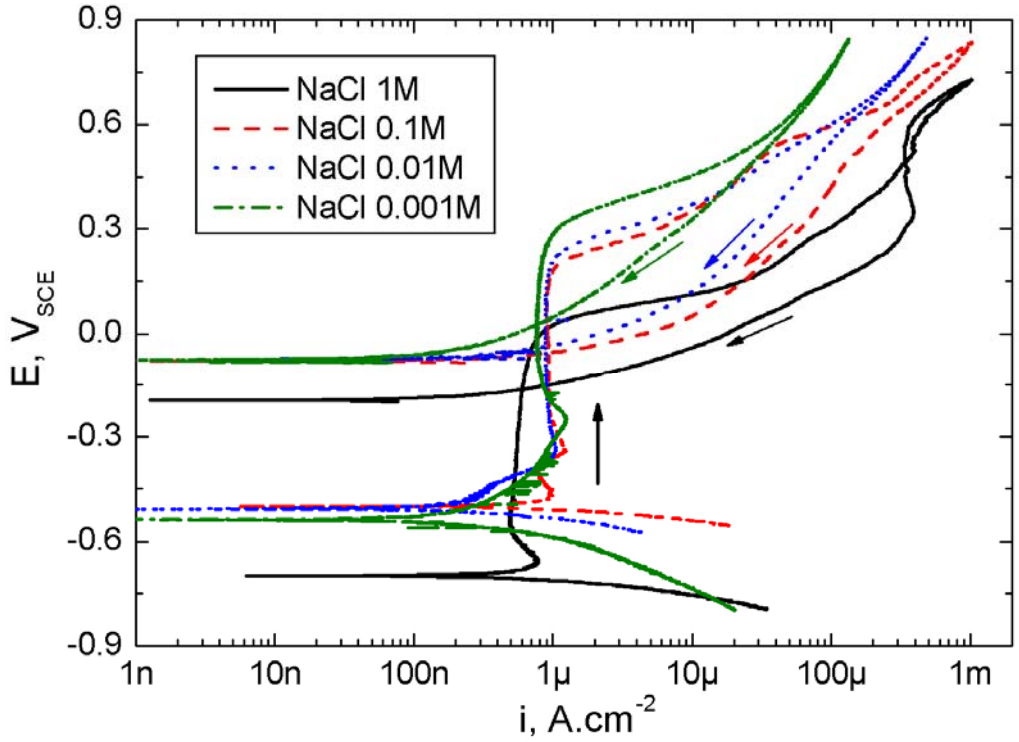

FIGURE 1: Cyclic Potentiodynamic Polarization (CPP) curves obtained for Alloy 22 in NaCl solutions of different concentrations at pH 6 and 90ºC.

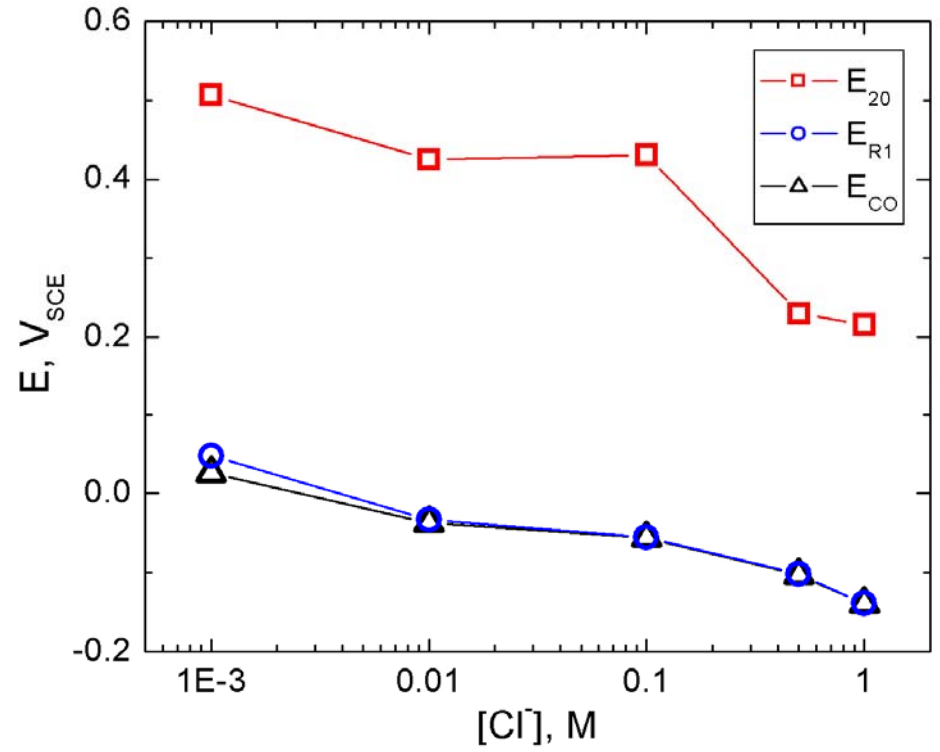

FIGURE 2: Critical parameters, breakdown (E_{20}) and repassivation (E_{R1} and E_{CO}) potentials, for Alloy 22 in NaCl solutions of different concentrations at pH 6 and 90ºC.

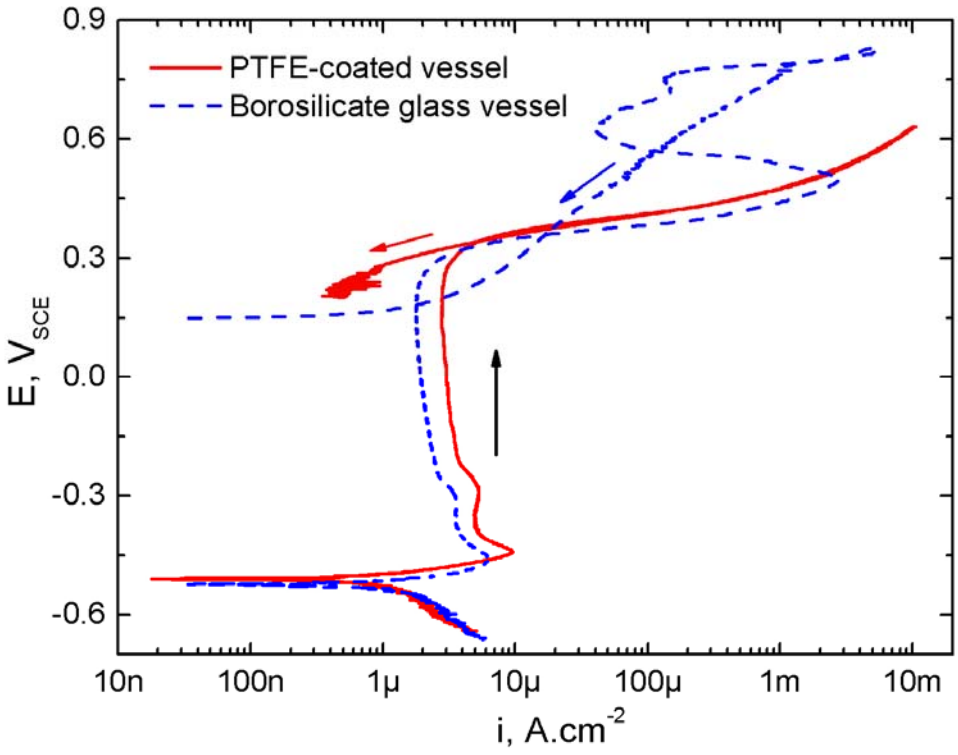

FIGURE 3: Cyclic Potentiodynamic Polarization (CPP) curves obtained for Alloy 22 in 1M NaF at pH 6 and 90ºC performed in the PTFE-coated vessel and in the borosilicate glass vessel.

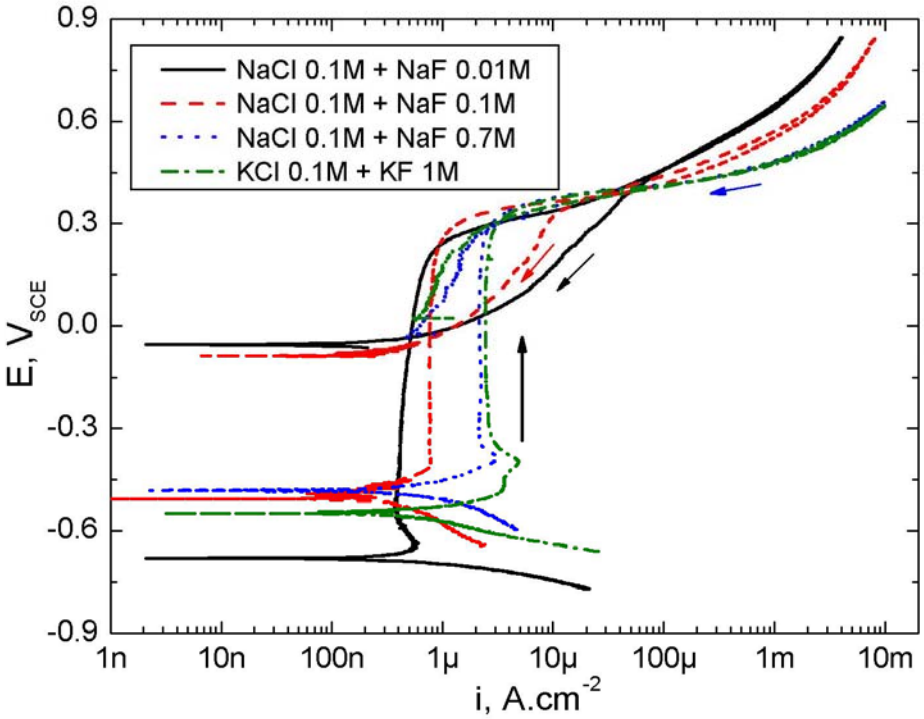

FIGURE 4: Cyclic Potentiodynamic Polarization (CPP) curves obtained for Alloy 22 in chloride plus fluoride solutions of different concentrations at pH 6 and 90ºC.

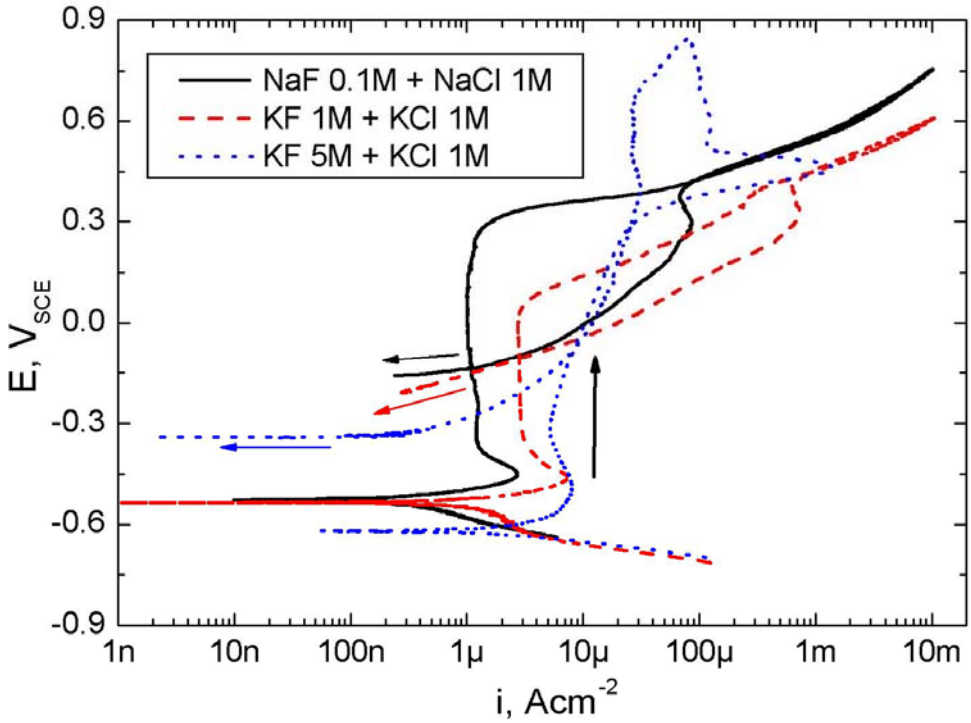

FIGURE 5: Cyclic Potentiodynamic Polarization (CPP) curves obtained for Alloy 22 in chloride plus fluoride solutions of different concentrations at pH 6 and 90ºC.

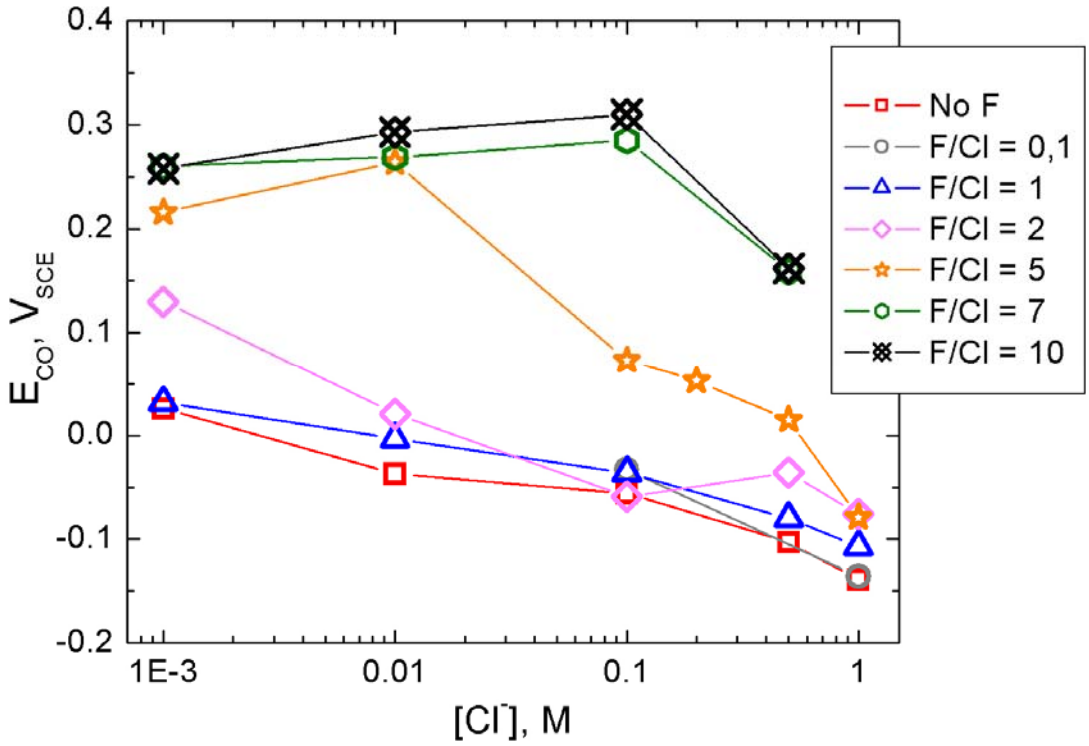

FIGURE 6: Cross over repassivation potential (E_{CO}) for Alloy 22 in chloride plus fluoride solutions of different concentrations at pH 6 and 90ºC.

FIGURE 7: Alloy 22 PCA specimen which suffered crevice corrosion after a CPP test in 1M NaCl solution at pH 6 and 90ºC.

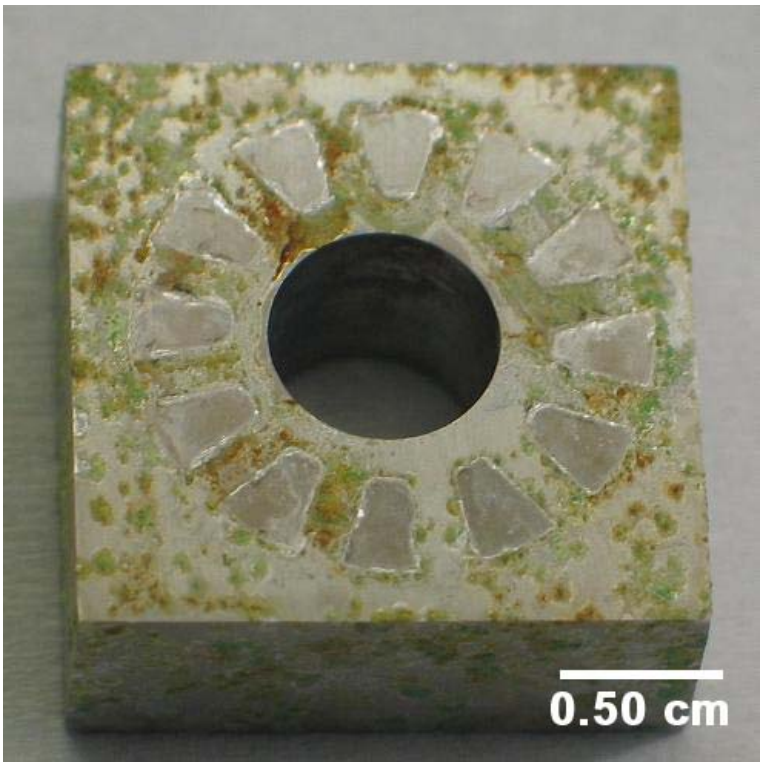

FIGURE 8: Alloy 22 PCA specimen which suffered crevice corrosion after a CPP test in 3.5M KF + 0.5M KCl solution at pH 6 and 90ºC.

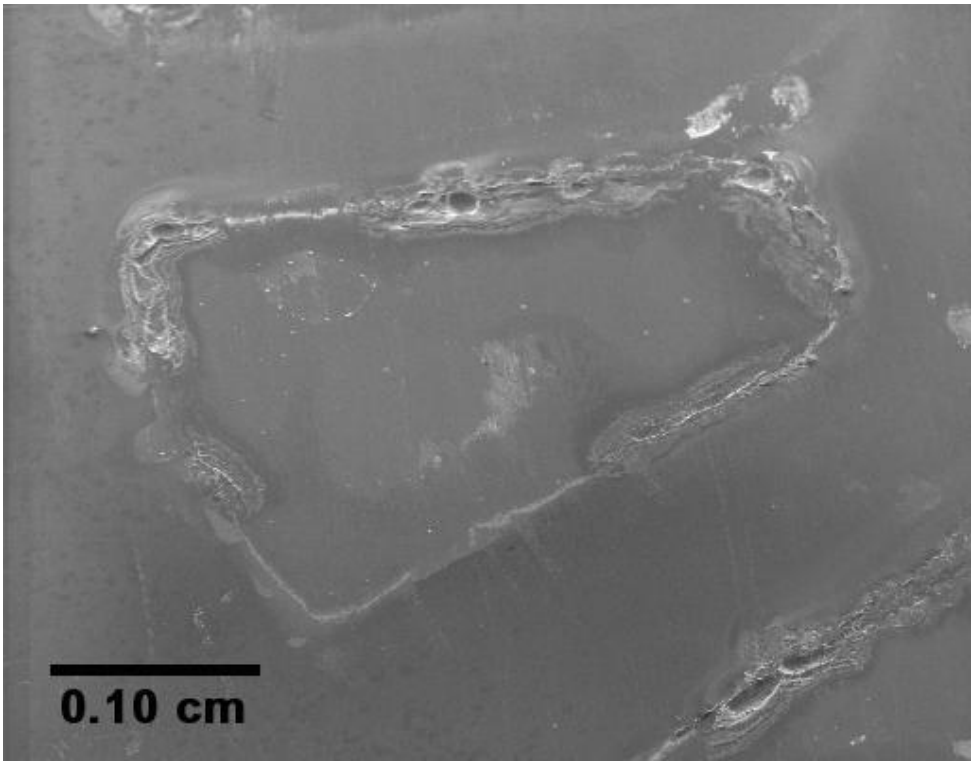

FIGURE 9: SEM micrograph showing crevice corrosion attack under a spot in a PCA specimen tested in 1M NaCl + 0.1M NaF at pH 6 and 90ºC. Magnification 32x.

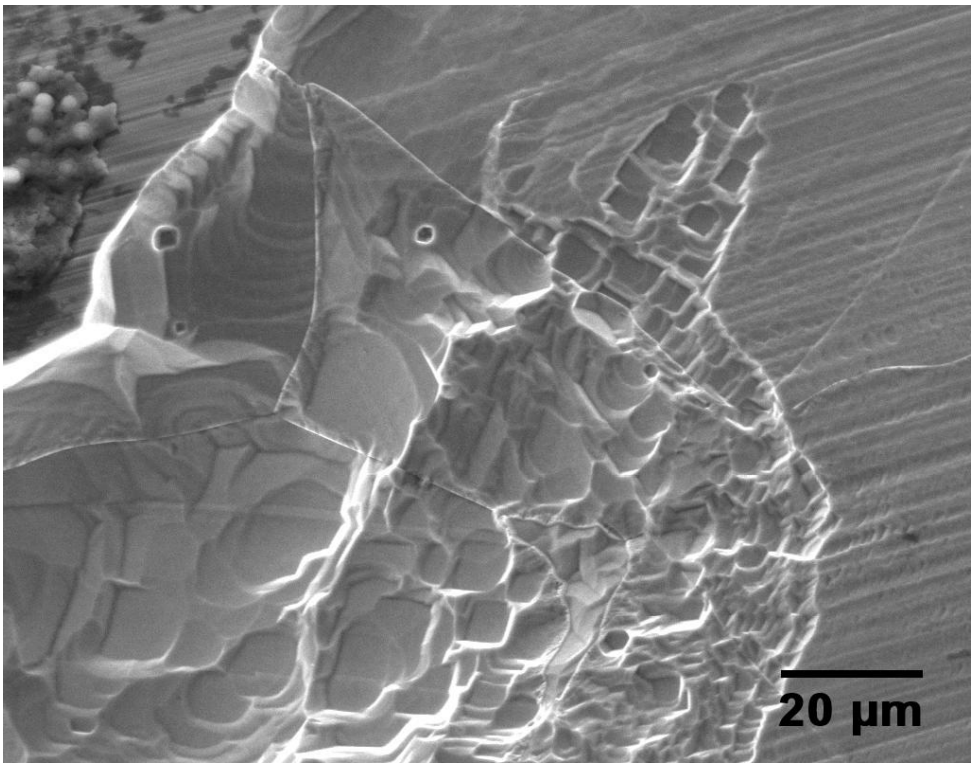

FIGURE 10: SEM micrograph showing crevice corrosion attack under a spot in a PCA specimen tested in 0.5M KCl + 1M NaF at pH 6 and 90ºC. Magnification 440x.

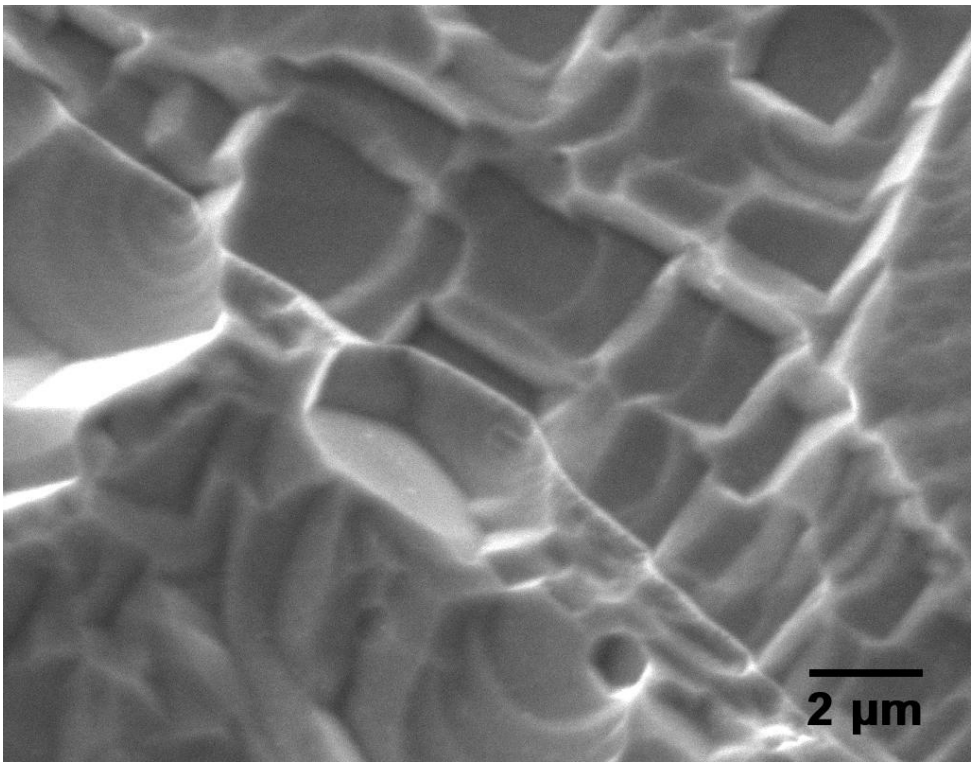

FIGURE 11: SEM micrograph showing crevice corrosion attack under a spot in a PCA specimen tested in 0.5M KCl + 1M NaF at pH 6 and 90ºC. Magnification 3500x.